

# Geophysical Research Letters

## RESEARCH LETTER

10.1029/2019GL085832

### Key Points:

- ENSO-like tropical Pacific decadal variability affects the relative frequency of El Niño and La Niña
- Frequency of ENSO events is modulated by decadal changes in the interbasin SST contrast and zonal winds over the western equatorial Pacific
- El Niño frequency is more sensitive to mean state changes than La Niña frequency due to their different onset mechanisms

### Supporting Information:

- Supporting Information S1

### Correspondence to:

T. Sun,  
tsun@edf.org

### Citation:

Sun, T., & Okumura, Y. M. (2020). Impact of ENSO-like tropical Pacific decadal variability on the relative frequency of El Niño and La Niña events. *Geophysical Research Letters*, 47, e2019GL085832. <https://doi.org/10.1029/2019GL085832>

Received 17 OCT 2019

Accepted 17 JAN 2020

Accepted article online 23 JAN 2020

## Impact of ENSO-Like Tropical Pacific Decadal Variability on the Relative Frequency of El Niño and La Niña Events

Tianyi Sun<sup>1,2</sup>  and Yuko M. Okumura<sup>1</sup> 

<sup>1</sup>Institute for Geophysics, Jackson School of Geosciences, University of Texas at Austin, Austin, TX, USA, <sup>2</sup>Now at Environmental Defense Fund, Austin, TX, USA

**Abstract** Observational and modeling studies show that the relative frequency of El Niño and La Niña varies in association with El Niño–Southern Oscillation (ENSO)-like tropical Pacific decadal variability (TPDV), but the causality of the linkage remains unclear. This study presents evidence that ENSO-like TPDV affects the frequency of ENSO events, particularly of El Niño, through a set of climate model experiments. During the positive phase of TPDV, tropical Pacific warming relative to the Indian and Atlantic Oceans increases the occurrence of anomalous westerly winds over the western equatorial Pacific in late boreal winter-spring, triggering more El Niño and fewer La Niña events. The opposite happens for the negative TPDV phase. The La Niña frequency is also influenced by oceanic adjustments following El Niño, which tends to counteract the effect of wind changes. The mean state control of ENSO offers a potential opportunity for decadal predictions of climate extremes.

**Plain Language Summary** Previous research shows that El Niño occurs more frequently than La Niña during decades when the tropical Pacific becomes warmer across the basin, and vice versa. However, it is not clear whether changes in the baseline conditions of the tropical Pacific are the cause or the effect of changes in the frequency of El Niño and La Niña. Using a set of climate model experiments, this study presents the evidence for the former case. In particular, basin-wide warming and cooling of the tropical Pacific are shown to strongly affect the frequency of El Niño by modulating surface winds over the western equatorial Pacific, which play an important role in triggering El Niño. The baseline conditions have less impact on the frequency of La Niña, for which slow oceanic processes are also important. These results may help to predict long-term changes in climate extremes over the regions strongly affected by El Niño and La Niña.

## 1. Introduction

The El Niño–Southern Oscillation (ENSO) arises from ocean-atmosphere interactions in the tropical Pacific and affects global weather patterns via atmospheric teleconnections (e.g., Alexander et al., 2002; Deser et al., 2017; McPhaden et al., 2010; Neelin et al., 1998; Timmermann et al., 2018; Trenberth et al., 1998). Previous studies suggest that many aspects of the ENSO vary on decadal-interdecadal time scales in association with changes in tropical Pacific mean climate (e.g., An & Jin, 2004; An & Wang, 2000; Ashok et al., 2007; Choi et al., 2012; Chung & Li, 2013; Guan & McPhaden, 2016; Hu & Fedorov, 2018; Kiem et al., 2003; Levine et al., 2017; Ogata et al., 2013; Trenberth & Hoar, 1996; Wang, 1995; Wittenberg, 2015; Ye & Hsieh, 2006). In particular, the amplitude, spatial pattern, frequency, and other properties of ENSO apparently changed in the late 1970s and 1990s with the regime shifts of ENSO-like tropical Pacific decadal variability (TPDV) that occurs as part of the interdecadal Pacific oscillation (IPO; Power et al., 1999). However, there is no consensus on what properties of ENSO vary with the IPO and what are the physical mechanisms of the linkages. For instance, some studies show that the ENSO amplitude is not significantly correlated with the IPO in observations (Yeh & Kirtman, 2005) and paleoclimate reconstructions (McGregor et al., 2010).

Observational evidence suggests that El Niño events become more frequent than La Niña events during the positive phase of IPO, and vice versa (Kiem et al., 2003; Verdon & Franks, 2006). This decadal variability in the relative frequency of El Niño and La Niña has been overlooked in previous studies, but recent modeling studies show that this is a robust feature of ENSO modulation that occurs with ENSO-like TPDV (Lin et al., 2018; Okumura, Sun & Wu, 2017). Okumura, Sun, and Wu (2017) suggest that ENSO-like TPDV affects the frequency of El Niño and La Niña events by modulating surface winds over the western equatorial Pacific.

However, it is difficult to determine the causality of their linkage, because decadal variations in ENSO properties may also leave a footprint on the mean state. In this study, we investigate the impact of ENSO-like TPDV on ENSO through a set of climate model experiments forced with surface heat flux anomalies associated with TPDV.

The rest of the paper is organized as follows. Section 2 describes the model experiments and definition of ENSO events. The simulated changes of ENSO properties and the associated atmospheric and oceanic mechanisms are reported in section 3. Section 4 provides summary and discussion.

## 2. Methodology

The model experiments are conducted with the Community Climate System Model Version 4 (CCSM4; Gent et al., 2011). The atmospheric component has a horizontal resolution of  $0.9^\circ$  latitude  $\times 1.25^\circ$  longitude with 26 levels in the vertical. The oceanic component has longitudinal spacing of  $1.13^\circ$  and latitudinal spacing varying from  $0.27^\circ$  at the equator to  $0.65^\circ$  at  $60^\circ\text{N/S}$  with 60 levels in the vertical. The CCSM4 simulates salient features of observed tropical Pacific mean climate and variability, including the asymmetry between El Niño and La Niña and diversity in the spatial patterns of ENSO sea surface temperature (SST) anomalies (Bellenger et al., 2014; Capotondi, 2013; Deser et al., 2012). Importantly, the relative frequency of El Niño and La Niña varies with ENSO-like TPDV in a 1300-year preindustrial control simulation of CCSM4 (hereafter CCSM4-CTL; Okumura, Sun, & Wu, 2017). As in observations, ENSO-like TPDV in CCSM4-CTL arises as the leading empirical orthogonal function of 10-year low-pass-filtered SST variability in the tropical Pacific ( $20^\circ\text{S}$  to  $20^\circ\text{N}$ ,  $120^\circ\text{E}$  to  $80^\circ\text{W}$ ; TPDV1; Figure 1a).

To examine the impact of ENSO-like TPDV on ENSO, we prescribe annual mean oceanic and atmospheric forcing associated with TPDV1 in CCSM4 ( $Q_F$ ; Figure 1b). Following Xie et al. (2010),  $Q_F$  is assumed to be in balance with Newtonian damping arising from temperature dependence of evaporation and estimated as

$$Q_F = \frac{L}{R_v \overline{T}^2} \overline{Q_{LH}} T',$$

where  $T$  is SST,  $Q_{LH}$  upward latent heat flux,  $L$  latent heat of evaporation, and  $R_v$  gas constant for water vapor, and the overbar and prime denote the climatology and anomaly, respectively. The SST anomaly associated with TPDV1 ( $T'$ ) is obtained by regressing 10-year low-pass-filtered SST on the leading principal component (PC1).  $Q_F$  is added to net surface heat flux in the tropical Pacific (linearly damped between  $20$ – $28^\circ\text{N/S}$ ) when the atmosphere is coupled to the ocean once a day.

We conduct two sets of experiments using  $Q_F$  for positive and negative two standard deviations of PC1 (TPDV1-P and TPDV1-N experiments). Both experiments consist of three ensemble members of 100-year simulations initialized with oceanic and atmospheric conditions from different years of the CCSM4-CTL. The surface heat flux forcing is sufficient to induce small changes in time mean SST in the tropical Pacific (up to  $\sim 0.3^\circ\text{C}$ ) but does not cause model drifts. Aside from adding constant surface heat flux forcing, the ocean and atmosphere are fully coupled to generate the ENSO. Additional sets of experiments are conducted using  $Q_F$  for positive and negative one standard deviation of PC1. The results are generally consistent with the TPDV1-P/N experiments, despite weaker response of the mean state and ENSO (Figures S1 and S2 in the supporting information).

We analyze the entire 100 years of the TPDV1-P/N experiments, although it takes about a decade for the equatorial ocean to adjust to surface heat flux forcing in the tropical Pacific (Sun & Okumura, 2019). Ocean-atmosphere anomalies in the TPDV1-P/N experiments are calculated relative to the climatology of the last 500 years of CCSM4-CTL. El Niño and La Niña events are defined when SST anomaly averaged in the Niño-3.4 region ( $5^\circ\text{N}$  to  $5^\circ\text{S}$ ,  $170^\circ\text{W}$  to  $120^\circ\text{W}$ ; hereafter the Niño-3.4 index) in December is greater than one standard deviation ( $1.26^\circ\text{C}$ ) and less than minus one standard deviation ( $-1.26^\circ\text{C}$ ), respectively. If the Niño-3.4 index satisfies the criterion for consecutive years, it is counted as a single event. Note that the Niño-3.4 index and ENSO anomalies include the forced response in the TPDV1-P/N experiments. We choose not to remove the forced response in the analysis of ENSO because of their strong interactive nature. Our choice is also relevant to real time observations, for which TPDV and ENSO cannot be distinguished. Further discussion is given on this issue in section 4. The statistical significance of ENSO changes in the TPDV1-P/N

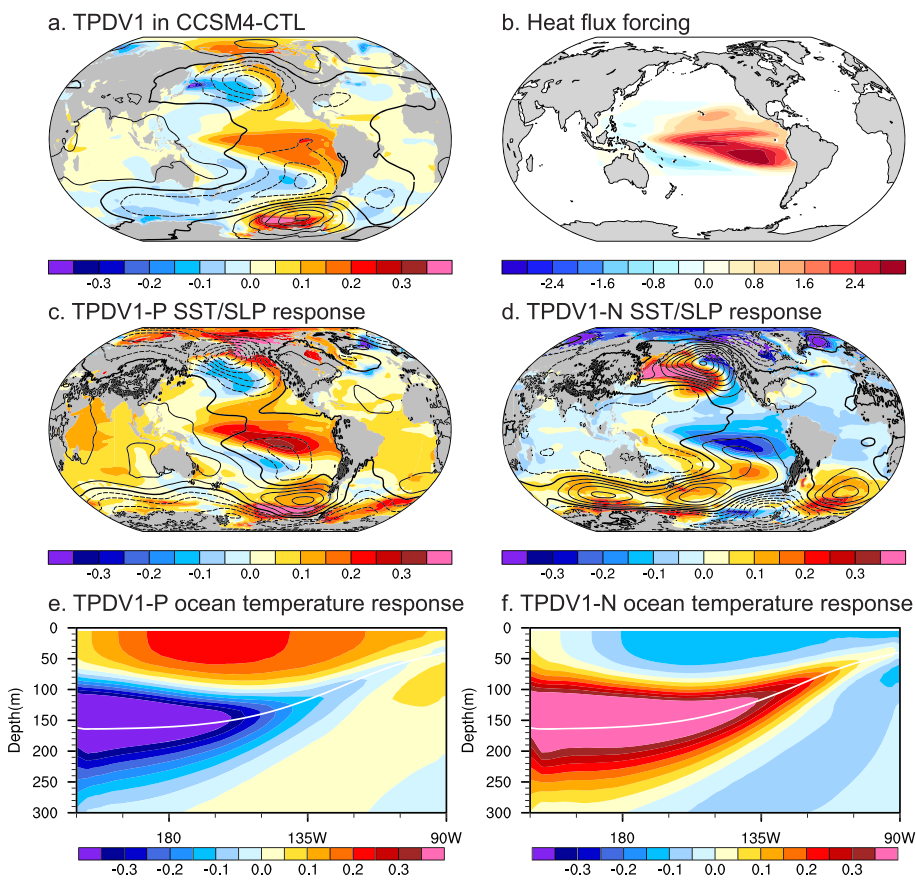


**Figure 1.** (a) Global ocean-atmosphere anomaly patterns associated with TPDV1 in CCSM4-CTL. Surface temperature (shading; °C) and sea level pressure (SLP; contours at intervals of 0.1 hPa) anomalies are regressed onto the standardized PC1. (b) Surface heat flux forcing ( $\text{W m}^{-2}$ ) used in the TPDV1-P experiment. The same forcing but with the opposite sign is used for the TPDV1-N experiment. (c–f) Ensemble mean annual response of (c, d) global surface temperature (shading; °C) and SLP (contours at intervals of 0.1 hPa) and (e, f) equatorial Pacific ( $3^{\circ}\text{N}$  to  $3^{\circ}\text{S}$ ) ocean potential temperature (shading; °C) in (c, e) the TPDV1-P and (d, f) TPDV1-N experiments. The white lines in (e) and (f) denote the climatological isopycnal  $\sigma_0 = 25.5 \text{ kg m}^{-3}$  that approximates the thermocline depth in CCSM4-CTL.

experiments is tested using a Monte-Carlo approach based on the CCSM4-CTL or a two-tailed Student's  $t$  test. The main conclusions of this study are not affected by excluding the first decade of the experiments or by modifying the definition of ENSO events.

### 3. Results

Although the surface heat flux forcing is applied only to the tropical Pacific in the TPDV1-P/N experiments, the annual mean ocean-atmosphere response exhibits global patterns, indicative of the role of atmospheric teleconnections (Figures 1c and 1d). For instance, the North Pacific shows SST anomalies opposite to those in the tropical Pacific in association with changes in the Aleutian low. The tropical Indian and Atlantic Oceans show SST anomalies of the same sign as in the tropical Pacific but with smaller amplitude. The global anomaly patterns closely resemble those associated with TPDV1 in CCSM4-CTL (Figure 1a). In addition to surface climate, the equatorial Pacific thermocline shoals and deepens in the TPDV1-P and TPDV1-N experiments, respectively, due to Sverdrup transport induced by atmospheric circulation anomalies over the tropical South Pacific (Figures 1e and 1f). The resultant subsurface ocean temperature anomalies act to weaken the forced mixed layer temperature anomalies through vertical temperature advection, especially in the central eastern equatorial Pacific where the thermocline is shallow. The annual mean ocean-atmosphere response is consistent among all ensemble members with small variations in the amplitude (Figure S3).

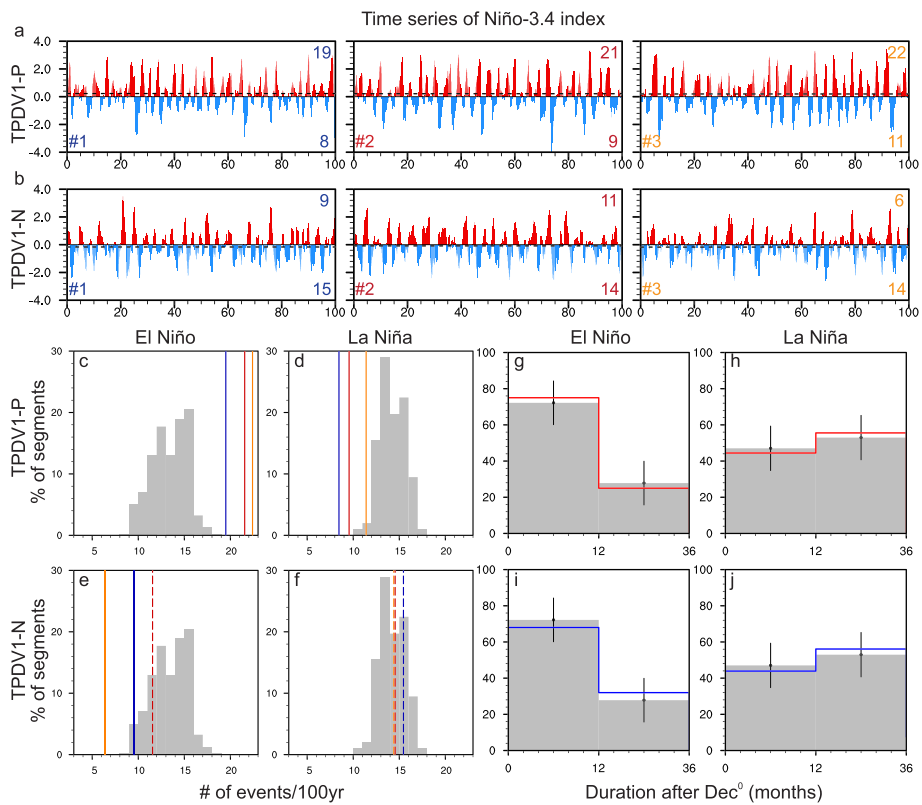


**Figure 2.** (a, b) Time series of the Niño-3.4 index ( $^{\circ}\text{C}$ ) in three ensemble members of (a) the TPDV1-P and (b) TPDV1-N experiments. Dashed lines denote mean changes in individual ensemble members. The numbers at the upper (lower) right corners indicate the numbers of El Niño (La Niña) events in individual ensemble members. (c–f) The numbers of (c, e) El Niño and (d, f) La Niña events in individual ensemble members of the (c, d) TPDV1-P and (e, f) TPDV1-N experiments (colored lines) compared to the histograms (%) based on 401 overlapping 100-year segments of the CCSM4-CTL (gray bars). The solid (dashed) lines indicate that the numbers of events in the experiments are outside (within) the 5–95% confidence intervals in the CCSM4-CTL. (g–j) Histograms (%) of (g, i) El Niño and (h, j) La Niña event duration in the (g, h) TPDV1-P and (i, j) TPDV1-N experiments (colored lines) and CCSM4-CTL (gray bars). The duration of El Niño (La Niña) event is defined as the number of months for which the Niño-3.4 index remains above 0.25 (below  $-0.25$ ) standard deviations of the monthly Niño-3.4 index after December of the first year. The error bars indicate the 5–95% confidence intervals in the CCSM4-CTL based on 1,000 randomly selected three 100-year segments.

The tropical Pacific ocean-atmosphere response shows distinct seasonality despite the constant forcing (Figures S4 and S5). In particular, equatorial SST anomalies peak in boreal winter and weaken from spring to summer, concurrently with eastward propagation of opposite subsurface ocean temperature anomalies. This seasonal propagation of subsurface temperature anomalies is associated with weakening of equatorial zonal wind anomalies in spring. The equatorial zonal wind anomalies retreat to the south of the equator in spring and expand into the tropical North Pacific in summer, following the seasonal migration of the inter-tropical convergence zone. Sun and Okumura (2019) suggest that zonal momentum advection by cross-equatorial winds plays an important role in the seasonality of equatorial zonal wind anomalies associated with TPDV.

Figure 2 compares ENSO properties in the TPDV1-P/N experiments with those in the CCSM4-CTL. The time series of the Niño-3.4 index clearly show that El Niño becomes more frequent than La Niña in the TPDV1-P experiment (Figure 2a) and La Niña becomes more frequent than El Niño in the TPDV1-N experiment (Figure 2b). These changes in the relative frequency of El Niño and La Niña are consistent with previous studies (Kiem et al., 2003; Lin et al., 2018; Okumura, Sun, & Wu, 2017; Verdon & Franks, 2006). Compared to the CCSM4-CTL, all three members of the TPDV1-P experiment have significantly more El Niño events and fewer La Niña events (Figures 2c and 2d). Two out of three members of the TPDV1-N experiment have significantly fewer El Niño events, but there is no apparent change in the number of La Niña events (Figures 2e and 2f). Although the analysis of CCSM4-CTL indicates that the frequency of multiyear El Niño events

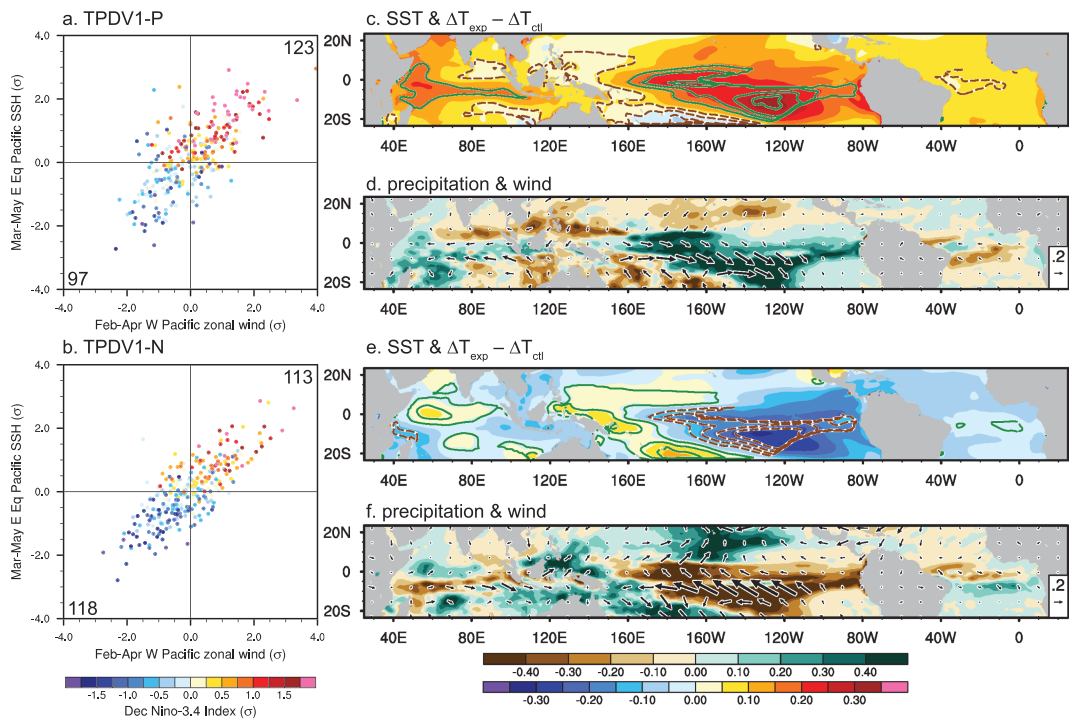


**Figure 3.** (a, b) Scatterplots of February–April surface zonal wind anomalies in the western equatorial Pacific ( $5^{\circ}\text{N}$  to  $5^{\circ}\text{S}$ ,  $130^{\circ}\text{E}$  to  $180^{\circ}\text{E}$ ) versus March–May SSH anomalies in the eastern equatorial Pacific ( $3^{\circ}\text{N}$  to  $3^{\circ}\text{S}$ ,  $150^{\circ}\text{W}$  to  $80^{\circ}\text{W}$ ) for (a) the TPDV1-P and (b) TPDV1-N experiments. The colors of dots indicate the values of the December Niño-3.4 index in the same year. All indices are standardized based on the mean and standard deviation of the same indices in the CCSM4-CTL. The numbers in the upper right and lower left corners indicate the numbers of points in these quadrants. (c–f) Maps of February–April mean changes in (c, e) SST (shading;  $^{\circ}\text{C}$ ) and  $\Delta T$  (contours at intervals of  $0.05\text{ }^{\circ}\text{C}$ ; negative contours dashed and zero contours omitted) and (d, f) precipitation (shading;  $\text{mm day}^{-1}$ ) and surface wind (vectors;  $\text{m s}^{-1}$ ) in (c, d) the TPDV1-P and (e, f) TPDV1-N experiments.

increases during the positive phase of TPDV1 (Okumura, Sun, & Wu, 2017), the duration of ENSO events does not change significantly in the TPDV1-P/N experiments (Figures 2g–2j). Neither does the ENSO amplitude, measured by standard deviation of the monthly Niño-3.4 index, change significantly in these experiments (not shown).

In both TPDV1-P/N experiments, the frequency of El Niño appears to be more sensitive to the mean state changes than the frequency of La Niña. This asymmetric modulation of El Niño and La Niña frequency may result from their different onset mechanisms. In the CCSM4-CTL, 96% of El Niño events develop from a neutral condition in the previous year, whereas 44% of La Niña events are preceded by El Niño (Table S1). The El Niño frequency changes in the TPDV1-P/N experiments come from the number of events developing from a neutral condition. The number of La Niña events developing from a neutral condition also decreases and increases in the TPDV1-P and TPDV1-N experiments, respectively. In the TPDV1-N experiment, however, this change is largely canceled out by a decrease in the number of La Niña preceded by El Niño, resulting in no apparent change in the total number of La Niña events. Thus, the frequency of La Niña is also controlled by the frequency of El Niño and attendant discharge of the equatorial oceanic heat content.

What causes the changes in the frequency of El Niño and La Niña events in the TPDV1-P/N experiments? In the CCSM4-CTL, the development of ENSO events tends to follow the emergence of surface zonal wind anomalies over the western equatorial Pacific in late boreal winter–spring and subsequent displacement of the thermocline in the eastern equatorial Pacific (Figure S6a). The same mechanism works in the TPDV1-P/N experiments and western Pacific zonal wind in February–April is strongly correlated with sea surface height (SSH; used as a proxy of the thermocline depth) in the eastern Pacific in March–May ( $r = 0.8$ ) and the Niño-3.4 index in December ( $r = 0.64$ ) of the same year (Figures 3a and 3b). Compared to the TPDV1-

N experiment, the TPDV1-P experiment shows more years of positive wind and SSH anomalies and fewer years of negative wind and SSH anomalies.

The surface wind anomalies leading to ENSO event development are, in turn, associated with anomalous interbasin SST contrast between the tropical Pacific and Indian/Atlantic Oceans in the CCSM4-CTL (Figure S6b). In the TPDV1-P experiment, mean SST increases over all tropical oceans during late boreal winter-spring, but the Pacific warms more than the Indian and Atlantic Oceans (Figure 3c). In the TPDV1-N experiment, the Pacific cools more than the Indian and Atlantic Oceans (Figure 3e). These mean changes in the interbasin SST contrast are comparable to those associated with ENSO event development in CCSM4-CTL (Figure S7). Over the tropical oceans, SST controls the atmospheric instability and convection tends to occur where SST exceeds the tropical mean value (Johnson & Xie, 2010). Here we define a positive SST deviation from the tropical mean value as

$$\Delta T = (T - T^*)H(T - T^*),$$

where  $T^*$  is the tropical mean SST and  $H$  is the Heaviside function (Okumura, 2019). The pattern of  $\Delta T$  anomalies explains the pattern of mean precipitation changes and associated surface winds in the TPDV1-P/N experiments (Figures 3c–3f). In the TPDV1-P experiment, the relative warming of the tropical Pacific increases precipitation over the central eastern Pacific and drives westerly winds over the western Pacific, leading to the increased frequency of El Niño. The TPDV1-N experiment shows opposite precipitation and wind changes.

It is noted that the patterns of mean precipitation changes are not perfectly symmetric between the two experiments and the TPDV1-N experiment shows a more meridional dipole pattern in the tropical Pacific. This asymmetry likely results from the presence of the equatorial Pacific cold tongue, which makes the cooling in the TPDV1-N experiment less effective in producing  $\Delta T$  anomalies than the warming in the TPDV1-P experiment. The associated wind changes show smaller zonal components over the western equatorial Pacific in the TPDV1-N than the TPDV1-P experiment, and this may explain why the TPDV1-N experiment exhibits less significant changes in the frequency of El Niño and La Niña (Figures 2c–2f). The meridional dipole pattern of ocean-atmosphere anomalies in this experiment may be further amplified by thermodynamic air-sea interactions as suggested by Xie et al. (2018).

To understand why the duration and amplitude of ENSO events do not change significantly in the TPDV1-P/N experiments, we compare the composite seasonal evolution of Niño-3.4 SST anomalies for El Niño and La Niña between the TPDV1-P/N experiments and CCSM4-CTL (Figure 4). The differences in the composite evolution are further decomposed into mean state changes and residuals that represent the impact of mean state changes on the ENSO dynamics. Neither experiment shows a significant change in the total seasonal evolution of El Niño and La Niña, except that La Niña is preceded by larger positive SST anomalies in the TPDV1-P experiment due to the increased fraction of La Niña preceded by El Niño (Table S1). The lack of changes in the seasonal ENSO event evolution in both experiments results from competing effects of mean state changes and their impacts on the ENSO dynamics. For example, the mean SST warming in the TPDV1-P experiment is largely counteracted by reduced El Niño warming and enhanced La Niña cooling (Figures 4e–4h), which are mostly caused by the mean thermocline shoaling (Figure 1e) and associated negative vertical ocean heat transport anomalies (Figure S8). Similarly, the mean SST cooling in the TPDV1-N experiment is counteracted by enhanced El Niño warming and reduced La Niña warming caused by the mean thermocline deepening (Figure 1f) and associated positive vertical ocean heat transport anomalies (Figure S8). Thus, the equatorial thermocline adjustments act as negative feedback to changes not only in the mean state but also in the ENSO event evolution. These effects, however, are not strong enough to interrupt the development of ENSO events caused by surface winds changes over the western Pacific.

#### 4. Summary and Discussion

Based on a suite of CCSM4 experiments, we show that mean state changes associated with ENSO-like TPDV modulate the relative frequency of El Niño and La Niña events. During the positive phase of TPDV, tropical Pacific warming relative to the Indian and Atlantic Oceans increases atmospheric deep convection over the central eastern Pacific in late boreal winter-spring. The associated increase in the occurrence of westerly

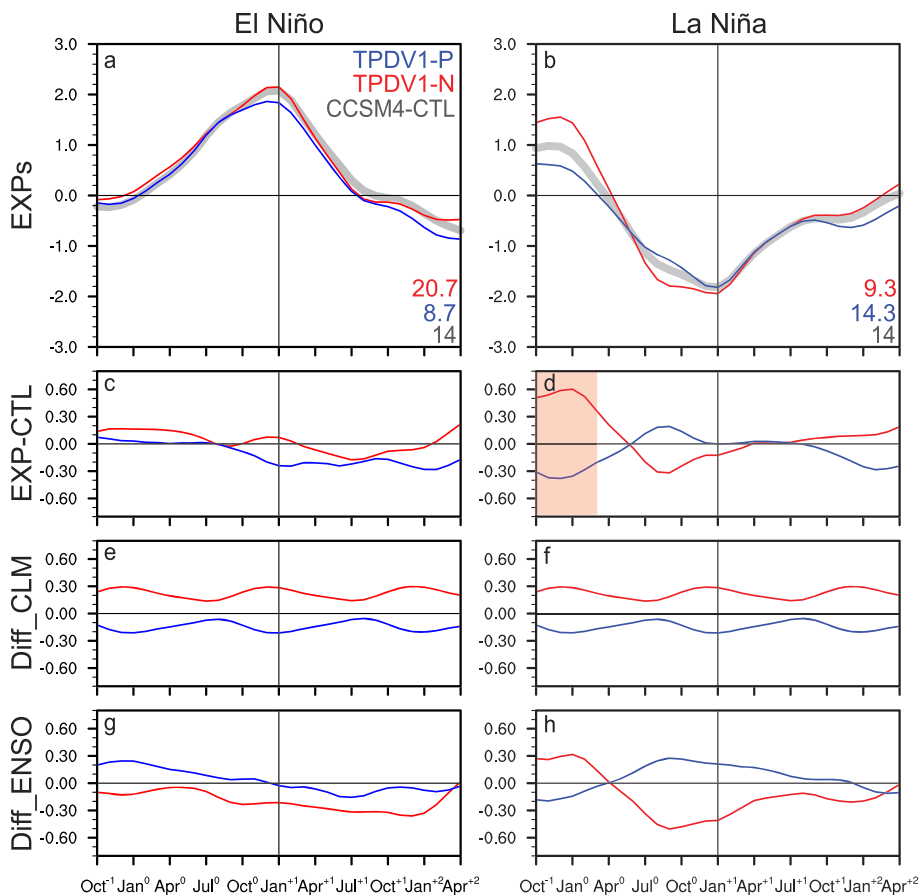


**Figure 4.** (a, b) Composite evolution of Niño-3.4 SST anomalies for (a) El Niño and (b) La Niña in the TPDV1-P (red) and TPDV1-N (blue) experiments and CCSM4-CTL (gray). The average numbers of El Niño and La Niña events per 100 years are indicated in the lower right. (c–h) Differences in (c) the El Niño and (d) La Niña composites between the TPDV1-P/N experiments and CCSM4-CTL (red/blue). These differences are further decomposed into (e, f) changes in the mean state and (g, h) residuals. The shading in (d) indicates where the TPDV1-P composite is significantly different from the CCSM4-CTL composite at the 95% confidence level based on a two-tailed Student's *t* test.

wind anomalies over the western equatorial Pacific leads to the development of more El Niño and fewer La Niña events. Conversely, tropical Pacific cooling during the negative phase of TPDV leads to the development of more La Niña and fewer El Niño events. The frequency of La Niña events is, however, also affected by changes in the frequency of El Niño and attendant oceanic adjustments, which tends to counteract the effects of wind changes. There are no significant changes in the duration and amplitude of ENSO events in these experiments due to competing effects of forced changes in mean SST and equatorial thermocline.

Changes in the frequency of ENSO events are closely related to changes in the tropical Pacific mean state in the TPDV1-P/N experiments. The TPDV1-P experiment, however, shows a significant increase of El Niño frequency even when ENSO events are defined based on the climatology of the experiment (Figure S9). Further research is needed to understand the nonlinear relationship between mean state and El Niño. One possible mechanism is state-dependent wind stress noise in the western equatorial Pacific (Hayashi & Watanabe, 2017; Kug et al., 2008; Levine & Jin, 2017; Thual et al., 2016). Westerly wind bursts and their eastward propagation, which affect the onset and growth of El Niño, exhibit dependency on the background SSTs. The relative warming of the tropical Pacific in the TPDV1-P experiment not only changes mean wind but may also enhance the state-dependent noise.

The changes in the relative frequency of El Niño and La Niña events simulated in our experiments are consistent with ENSO modulations associated with the IPO in observations (Kiem et al., 2003; Verdon & Franks,

2006) and climate models (Lin et al., 2018; Okumura, Sun, & Wu, 2017). Since changes in the ENSO event frequency would in turn induce ENSO-like mean state changes, previous studies could not distinguish the cause and effect. Our study provides the evidence that ENSO-like TPDV affects the ENSO event frequency. The effect of TPDV on the duration and amplitude of ENSO events may be underestimated in our experiments, in which the equatorial thermocline equilibrates with surface wind changes driven by surface heat flux forcing. Previous studies show that it takes up to a decade for the equatorial thermocline to adjust to surface wind changes associated with TPDV, which may lead to the phase reversal of TPDV in observations and unforced model simulations (Chang et al., 2001; Giese, 2002; Hasegawa et al., 2007; Luo et al., 2003; Luo & Yamagata, 2001; Sun & Okumura, 2019; Tatebe et al., 2013).

The findings of this study have important implications for decadal predictions of climate extremes over the regions strongly affected by the ENSO. For example, more frequent La Niña events would increase the occurrence of drought in the southern and western US (e.g., Cook et al., 2007; Dai et al., 1998; Okumura DiNezio, & Deser, 2017; Seager & Hoerling, 2014), while more frequent El Niño events would increase the occurrence of drought in northern and eastern Australia (e.g., Allan, 1988; McBride & Nicholls, 1983; Ropelewski & Halpert, 1987) and southern Africa (e.g., Lindesay, 1988; Ogutu & Owen-Smith, 2003). Knowing the potential changes in ENSO statistics in the coming decades is critical for agricultural and water resource planning (Anderson et al., 2017, 2018; Iizumi et al., 2014). The current generation of climate models, however, has lower decadal predictive skills in the central tropical and North Pacific compared to the North Atlantic and Indian Oceans (e.g., Guemas et al., 2012; Kim et al., 2012; Meehl et al., 2014; Meehl & Teng, 2014; Newman, 2013; van Oldenborgh et al., 2012). The lack of predictive skills may result from insufficient understanding of both the IPO and its relation to the ENSO. Our model experiments suggest strong interactions between the IPO and ENSO, which could help sustain the phase of IPO, whereas the delayed oceanic adjustments provide a negative feedback. These mechanisms need to be validated further in observations before we could improve our decadal climate predictions.

## Acknowledgments

The CCSM4 control simulation was conducted and made available to the public by the CESM working groups. The authors thank Xian Wu, Martin Puy, Pedro DiNezio, Noel Keenlyside, Amy Clement, and participants of the CLIVAR TPDV workshops for helpful discussions and Nan Rosenbloom and Muhammed Shaikh for their assistance with the CCSM4 experiments.

Insightful comments from two anonymous reviewers helped to improve the manuscript. This work was supported by the NSF Climate and Large-Scale Dynamics Program (AGS-1302346) and the NOAA Climate Program Office Modeling, Analysis, Predictions, and Projections Program (NA17OAR4310149). T. Sun was partially supported by the Ewing-Worzel Fellowship at Institute for Geophysics, University of Texas at Austin. Data used in this study are available at Sun & Okumura, 2019, "Replication Data for: Impact of ENSO-like tropical Pacific decadal variability on the relative frequency of El Niño and La Niña events" (10.18738/T8/XD8GGI) Texas Data Repository Dataverse, V1.

## References

- Alexander, M. A., Bladé, I., Newman, M., Lanzante, J. R., Lau, N.-C., & Scott, J. D. (2002). The atmospheric bridge: The influence of ENSO teleconnections on air-sea interaction over the global oceans. *Journal of Climate*, 15(16), 2205–2231. [http://doi.org/10.1175/1520-0442\(2002\)015<2205:TABTIO>2.0.CO;2](http://doi.org/10.1175/1520-0442(2002)015<2205:TABTIO>2.0.CO;2)
- Allan, R. J. (1988). El Niño Southern Oscillation influences in the Australasian region. *Progress in Physical Geography: Earth and Environment*, 12(3), 313–348. <http://doi.org/10.1177/030913338801200301>
- An, S.-I., & Jin, F.-F. (2004). Nonlinearity and asymmetry of ENSO. *Journal of Climate*, 17(12), 2399–2412. [http://doi.org/10.1175/1520-0442\(2004\)017<2399:NAAOE>2.0.CO;2](http://doi.org/10.1175/1520-0442(2004)017<2399:NAAOE>2.0.CO;2)
- An, S.-I., & Wang, B. (2000). Interdecadal change of the structure of the ENSO mode and its impact on the ENSO frequency. *Journal of Climate*, 13(12), 2044–2055. [http://doi.org/10.1175/1520-0442\(2000\)013<2044:ICOTSO>2.0.CO;2](http://doi.org/10.1175/1520-0442(2000)013<2044:ICOTSO>2.0.CO;2)
- Anderson, W., Seager, R., Baethgen, W., & Cane, M. A. (2017). Crop production variability in North and South America forced by life-cycles of the El Niño Southern Oscillation. *Agricultural and Forest Meteorology*, 239, 151–165. <https://doi.org/10.1016/j.agrformet.2017.03.008>
- Anderson, W., Seager, R., Baethgen, W., & Cane, M. A. (2018). Trans-Pacific ENSO teleconnections pose a correlated risk to agriculture. *Agricultural and Forest Meteorology*, 262, 298–309. <https://doi.org/10.1016/j.agrformet.2018.07.023>
- Ashok, K., Behera, S. K., Rao, S. A., Weng, H., & Yamagata, T. (2007). El Niño Modoki and its possible teleconnection. *Journal of Geophysical Research*, 112, C11007. <http://doi.org/10.1029/2006JC003798>
- Bellenger, H., Guiyadi, E., Leloup, J., Lengaigne, M., & Vialard, J. (2014). ENSO representation in climate models: From CMIP3 to CMIP5. *Climate Dynamics*, 42(7–8), 1999–2018. <http://doi.org/10.1007/s00382-013-1783-z>
- Capotondi, A. (2013). ENSO diversity in the NCAR CCSM4 climate model. *Journal of Geophysical Research: Oceans*, 118, 4755–4770. <http://doi.org/10.1002/jgrc.20335>
- Chang, P., Giese, B. S., Ji, L., Seidel, H. F., & Wang, F. (2001). Decadal change in the south tropical Pacific in a Global Assimilation Analysis. *Geophysical Research Letters*, 28(18), 3461–3464. <http://doi.org/10.1029/2001GL013018>
- Choi, J., An, S.-I., & Yeh, S.-W. (2012). Decadal amplitude modulation of two types of ENSO and its relationship with the mean state. *Climate Dynamics*, 38(11–12), 2631–2644. <https://doi.org/10.1007/s00382-011-1186-y>
- Chung, P.-H., & Li, T. (2013). Interdecadal relationship between the mean state and El Niño types. *Journal of Climate*, 26(2), 361–379. <http://doi.org/10.1175/JCLI-D-12-00106.1>
- Cook, E. R., Seager, R., Cane, M. A., & Stahle, D. W. (2007). North American drought: Reconstructions, causes, and consequences. *Earth-Science Reviews*, 81(1–2), 93–134. <http://doi.org/10.1016/j.earscirev.2006.12.002>
- Dai, A., Trenberth, K. E., & Karl, T. R. (1998). Global variations in droughts and wet spells: 1900–1995. *Geophysical Research Letters*, 25(17), 3367–3370. <http://doi.org/10.1029/98GL52511>
- Deser, C., Guo, R., & Lehner, F. (2017). The relative contributions of tropical Pacific sea surface temperatures and atmospheric internal variability to the recent global warming hiatus. *Geophysical Research Letters*, 44, 7945–7954. <http://doi.org/10.1002/2017gl074273>
- Deser, C., Phillips, A. S., Tomas, R. A., Okumura, Y. M., Alexander, M. A., Capotondi, A., et al. (2012). ENSO and Pacific decadal variability in the Community Climate System Model version 4. *Journal of Climate*, 25(8), 2622–2651. <http://doi.org/10.1175/JCLI-D-11-00301.1>
- Gent, P. R., Danabasoglu, G., Donner, L. J., Holland, M. M., Hunke, E. C., Jayne, S. R., et al. (2011). The Community Climate System Model version 4. *Journal of Climate*, 24(19), 4973–4991. <http://doi.org/10.1175/2011JCLI4083.1>

- Giese, B. S. (2002). Southern hemisphere origins of the 1976 climate shift. *Geophysical Research Letters*, 29(2), 1687. <http://doi.org/10.1029/2001GL013268>
- Guan, C., & McPhaden, M. J. (2016). Ocean processes affecting the twenty-first-century shift in ENSO SST variability. *Journal of Climate*, 29(19), 6861–6879. <http://doi.org/10.1175/JCLI-D-15-0870.1>
- Guemas, V., Doblas-Reyes, F. J., Lienert, F., Soufflet, Y., & Du, H. (2012). Identifying the causes of the poor decadal climate prediction skill over the North Pacific. *Journal of Geophysical Research*, 117, D20111. <http://doi.org/10.1029/2012JD018004>
- Hasegawa, T., Yasuda, T., & Hanawa, K. (2007). Generation mechanism of quasidecadal variability of upper ocean heat content in the equatorial Pacific Ocean. *Journal of Geophysical Research*, 112, C08012. <https://doi.org/10.1029/2006JC003755>
- Hayashi, M., & Watanabe, M. (2017). ENSO complexity induced by state dependence of westerly wind events. *Journal of Climate*, 30(9), 3401–3420. <http://doi.org/10.1175/JCLI-D-16-0406.1>
- Hu, S., & Fedorov, A. V. (2018). Cross-equatorial winds control El Niño diversity and change. *Nature Climate Change*, 8(9), 798. <https://doi.org/10.1038/s41558-018-0248-0>
- Iizumi, T., Luo, J.-J., Challinor, A. J., Sakurai, G., Yokozawa, M., Sakuma, H., et al. (2014). Impacts of El Niño Southern Oscillation on the global yields of major crops. *Nature Communications*, 5(1), 3712. <http://doi.org/10.1038/ncomms4712>
- Johnson, N. C., & Xie, S.-P. (2010). Changes in the sea surface temperature threshold for tropical convection. *Nature Geoscience*, 3(12), 842–845.
- Kiem, A. S., Franks, S. W., & Kuczera, G. (2003). Multi-decadal variability of flood risk. *Geophysical Research Letters*, 30(2), 1035. <http://doi.org/10.1029/2002GL015992>
- Kim, H.-M., Webster, P. J., & Curry, J. A. (2012). Evaluation of short-term climate change prediction in multi-model CMIP5 decadal hindcasts. *Geophysical Research Letters*, 39, L10701. <http://doi.org/10.1029/2012GL051644>
- Kug, J.-S., Jin, F.-F., Sooraj, K. P., & Kang, I.-S. (2008). State-dependent atmospheric noise associated with ENSO. *Geophysical Research Letters*, 35, L05701. <https://doi.org/10.1029/2007GL032017>
- Levine, A., & Jin, F.-F. (2017). A simple approach to quantifying the noise–ENSO interaction. Part I: Deducing the state-dependency of the windstress forcing using monthly mean data. *Climate Dynamics*, 48(1), 1–18. <https://doi.org/10.1007/s00382-015-2748-1>
- Levine, A. F., McPhaden, M. J., & Frierson, D. M. (2017). The impact of the AMO on multidecadal ENSO variability. *Geophysical Research Letters*, 44, 3877–3886. <https://doi.org/10.1002/2017GL072524>
- Lin, R., Zheng, F., & Dong, X. (2018). ENSO frequency asymmetry and the Pacific decadal oscillation in observations and 19 CMIP5 models. *Advances in Atmospheric Sciences*, 35(5), 495–506. <http://doi.org/10.1007/s00376-017-7133-z>
- Lindesay, J. A. (1988). South African rainfall, the Southern Oscillation and a Southern Hemisphere semi-annual cycle. *Journal of Climatology*, 8(1), 17–30. <http://doi.org/10.1002/joc.3370080103>
- Luo, J.-J., Masson, S., Behera, S. K., Delecluse, P., Gualdi, S., Navarra, A., & Yamagata, T. (2003). South Pacific origin of the decadal ENSO-like variation as simulated by a coupled GCM. *Geophysical Research Letters*, 30(24), 2250. <http://doi.org/10.1029/2003GL018649>
- Luo, J.-J., & Yamagata, T. (2001). Long-term El Niño–Southern Oscillation (ENSO)-like variation with special emphasis on the South Pacific. *Journal of Geophysical Research*, 106(C10), 22,211–22,227. <http://doi.org/10.1029/2000jc000471>
- McBride, J. L., & Nicholls, N. (1983). Seasonal relationships between Australian rainfall and the Southern Oscillation. *Monthly Weather Review*, 111(10), 1998–2004. [http://doi.org/10.1175/1520-0493\(1983\)111<1998:SRBARA>2.0.CO;2](http://doi.org/10.1175/1520-0493(1983)111<1998:SRBARA>2.0.CO;2)
- McGregor, S., Timmermann, A., & Timm, O. (2010). A unified proxy for ENSO and PDO variability since 1650. *Climate of the Past*, 6(1), 1–17. <http://doi.org/10.5194/cp-6-1-2010>
- McPhaden, M. J., Busalacchi, A. J., & Anderson, D. L. T. (2010). A TOGA retrospective. *Oceanography*, 23(3), 86–103. <https://doi.org/10.5670/oceanog.2010.26>
- Meehl, G. A., Goddard, L., Boer, G., Burgman, R., Branstator, G., Cassou, C., et al. (2014). Decadal climate prediction: An update from the trenches. *Bulletin of the American Meteorological Society*, 95(2), 243–267. <http://doi.org/10.1175/BAMS-D-12-00241.1>
- Meehl, G. A., & Teng, H. (2014). CMIP5 multi-model hindcasts for the mid-1970s shift and early 2000s hiatus and predictions for 2016–2035. *Geophysical Research Letters*, 41, 1711–1716. <http://doi.org/10.1002/2014GL059256>
- Neelin, D. J., Battisti, D. S., Hirst, A. C., Jin, F.-F., Wakata, Y., Yamagata, T., & Zebiak, S. E. (1998). ENSO theory. *Journal of Geophysical Research*, 103(C7), 14,261–14,290. <http://doi.org/10.1029/97JC03424>
- Newman, M. (2013). An empirical benchmark for decadal forecasts of global surface temperature anomalies. *Journal of Climate*, 26(14), 5260–5269. <http://doi.org/10.1175/JCLI-D-12-00590.1>
- Ogata, T., Xie, S.-P., Wittenberg, A., & Sun, D. Z. (2013). Interdecadal amplitude modulation of El Niño–Southern Oscillation and its impact on tropical Pacific decadal variability. *Journal of Climate*, 26(18), 7280–7297. <https://doi.org/10.1175/JCLI-D-12-00415.1>
- Ogutu, J. O., & Owen-Smith, N. (2003). ENSO, rainfall and temperature influences on extreme population declines among African savanna ungulates. *Ecology Letters*, 6(5), 412–419. <http://doi.org/10.1046/j.1461-0248.2003.00447.x>
- Okumura, Y. M. (2019). ENSO diversity from an atmospheric perspective. *Current Climate Change Reports*, 2, 1–13. <http://doi.org/10.1007/s40641-019-00138-7>
- Okumura, Y. M., DiNezio, P., & Deser, C. (2017). Evolving impacts of multiyear La Niña events on atmospheric circulation and U.S. drought. *Geophysical Research Letters*, 44, 11,614–11,623. <http://doi.org/10.1002/2017GL075034>
- Okumura, Y. M., Sun, T., & Wu, X. (2017). Asymmetric modulation of El Niño and La Niña and the linkage to tropical Pacific decadal variability. *Journal of Climate*, 30(12), 4705–4733. <https://doi.org/10.1175/jcli-d-16-0680.1>
- Power, S., Casey, T., Folland, C., Colman, A., & Mehta, V. (1999). Inter-decadal modulation of the impact of ENSO on Australia. *Climate Dynamics*, 15(5), 319–324. <https://doi.org/10.1007/s003820050284>
- Ropelewski, C. F., & Halpert, M. S. (1987). Global and regional scale precipitation patterns associated with the El Niño/Southern Oscillation. *Monthly Weather Review*, 115(8), 1606–1626. [http://doi.org/10.1175/1520-0493\(1987\)115<1606:GARSPPP>2.0.CO;2](http://doi.org/10.1175/1520-0493(1987)115<1606:GARSPPP>2.0.CO;2)
- Seager, R., & Hoerling, M. (2014). Atmosphere and ocean origins of North American droughts. *Journal of Climate*, 27(12), 4581–4606. <http://doi.org/10.1175/JCLI-D-13-00329.1>
- Sun, T., & Okumura, Y. M. (2019). Role of stochastic atmospheric forcing from the South and North Pacific in tropical Pacific decadal variability. *Journal of Climate*, 32(13), 4013–4038. <http://doi.org/10.1175/JCLI-D-18-0536.1>
- Tatebe, H., Imada, Y., Mori, M., Kimoto, M., & Hasumi, H. (2013). Control of decadal and bidecadal climate variability in the tropical Pacific by the off-equatorial South Pacific Ocean. *Journal of Climate*, 26(17), 6524–6534. <http://doi.org/10.1175/JCLI-D-12-00137.1>
- Thual, S., Majda, A. J., Chen, N., & Stechmann, S. N. (2016). Simple stochastic model for El Niño with westerly wind bursts. *Proceedings of the National Academy of Sciences*, 113(37), 10,245–10,250. <http://doi.org/10.1029/2006JC003798>
- Timmermann, A., An, S.-I., Kug, J.-S., Jin, F.-F., Cai, W., Capotondi, A., et al. (2018). El Niño–Southern Oscillation complexity. *Nature*, 559 (7715), 535–545. <http://doi.org/10.1038/s41586-018-0252-6>

- Trenberth, K. E., Branstator, G. W., Karoly, D., Kumar, A., Lau, N.-C., & Ropelewski, C. (1998). Progress during TOGA in understanding and modeling global teleconnections associated with tropical sea surface temperatures. *Journal of Geophysical Research*, 103(C7), 14,291–14,324. <http://doi.org/10.1029/97JC01444>
- Trenberth, K. E., & Hoar, T. J. (1996). The 1990–1995 El Niño–Southern Oscillation event: Longest on record. *Geophysical Research Letters*, 23(1), 57–60. <http://doi.org/10.1029/95GL03602>
- van Oldenborgh, G. J., Doblas-Reyes, F. J., Wouters, B., & Hazeleger, W. (2012). Decadal prediction skill in a multi-model ensemble. *Climate Dynamics*, 38(7), 1263–1280.
- Verdon, D. C., & Franks, S. W. (2006). Long-term behaviour of ENSO: Interactions with the PDO over the past 400 years inferred from paleoclimate records. *Geophysical Research Letters*, 33(6), 2331. <http://doi.org/10.1029/2005GL025052>
- Wang, B. (1995). Interdecadal changes in El Niño onset in the last four decades. *Journal of Climate*, 8(2), 267–285. [http://doi.org/10.1175/1520-0442\(1995\)008<0267:ICENO>2.0.CO;2](http://doi.org/10.1175/1520-0442(1995)008<0267:ICENO>2.0.CO;2)
- Wittenberg, A. T. (2015). Low-frequency variations of ENSO. *U.S. CLIVAR Variations*, 13(1), 26–31.
- Xie, S.-P., Deser, C., Vecchi, G. A., Ma, J., Teng, H., & Wittenberg, A. T. (2010). Global Warming Pattern Formation: Sea Surface Temperature and Rainfall. *Journal of Climate*, 23(4), 966–986. <https://doi.org/10.1175/2009jcli3329.1>
- Xie, S.-P., Peng, Q., Kamae, Y., Zheng, X.-T., Tokinaga, H., & Wang, D. (2018). Eastern Pacific ITCZ dipole and ENSO diversity. *Journal of Climate*, 31(11), 4449–4462. <http://doi.org/10.1175/JCLI-D-17-0905.1>
- Ye, Z., & Hsieh, W. W. (2006). The influence of climate regime shift on ENSO. *Climate Dynamics*, 26(7–8), 823–833. <http://doi.org/10.1007/s00382-005-0105-5>
- Yeh, S.-W., & Kirtman, B. P. (2005). Pacific decadal variability and decadal ENSO amplitude modulation. *Geophysical Research Letters*, 32, L05703. <http://doi.org/10.1029/2004GL021731>